

# Constraints on the generalized tachyon field models from latest observational data

Rong-Jia Yang<sup>1\*</sup>, Shuang Nan Zhang<sup>1,2,3</sup>, and Yuan Liu<sup>1</sup>

<sup>1</sup> *Department of Physics and Tsinghua Center for Astrophysics,  
Tsinghua University, Beijing 100084, China*

<sup>2</sup> *Key Laboratory of Particle Astrophysics,  
Institute of High Energy Physics, Chinese Academy of Sciences,  
P.O. Box 918-3, Beijing 100049, China,*

<sup>3</sup> *Physics Department, University of Alabama in Huntsville, Huntsville, AL 35899, USA*

## Abstract

We consider constraints on generalized tachyon field (GTF) models from latest observational data (including 182 gold SNIa data, the shift parameter, and the acoustic scale). We obtain at 68.3% confidence level  $\Omega_m = 0.37 \pm 0.01$ ,  $k_0 = 0.09^{+0.04}_{-0.03}$ ,  $\alpha = 1.8^{+7.4}_{-0.7}$  (the best-fit values of the parameters) and  $z_{q=0} \sim 0.47 - 0.51$  (the transitional redshift) for GTF as dark energy component only;  $k_0 = 0.21^{+0.20}_{-0.18}$ ,  $\alpha = 0.57 \pm 0.01$  and  $z_{q=0} \sim 0.49 - 0.68$  for GTF as unification of dark energy and dark matter. In both cases, GTF evolves like dark matter in the early universe. By applying model-comparison statistics and test with independent  $H(z)$  data, we find GTF dark energy scenario is favored over the  $\Lambda$ CDM model, and the  $\Lambda$ CDM model is favored over GTF unified dark matter by the combined data. For GTF as dark energy component, the fluctuations of matter density is consistent with the growth of linear density perturbations. For GTF unified dark matter, the growth of GTF density fluctuations grow more slowly for  $a \rightarrow 1$ , meaning GTF do not behave as classical  $\Lambda$ CDM scenarios.

PACS numbers: 95.36.+x, 98.80.-k, 98.80.Es

---

\* yangrj05@mails.tsinghua.edu.cn

## I. INTRODUCTION

Tachyon field can be seen as special cases of k-essence [1] and has been explored extensively [2, 3, 4, 5, 6, 7, 8, 9, 10, 11, 12, 13, 14]. For a constant potential, the tachyon field can be generalized as

$$F(X) = -V_0(1 - 2X^n)^{\frac{1}{2n}}, \quad (1)$$

called generalized tachyon field (GTF) [15], where  $n$  is a non-zero parameter. Such model can be considered as a scalar field realization of the generalized Chaplygin gas (GCG) [15, 16, 17, 18]. With the theoretical constraint on purely kinetic k-essence:  $F_x = F_0 a^{-3}$ , where  $F_0$  is a constant [15, 19, 20], one gets the expressions for the equation of state parameter (EoS)  $w_k$  and the sound speed  $c_s^2$  of the GTF depending on the scale factor (so the redshift) respectively

$$w_k = -\frac{1}{1 + 2k_0^{2\alpha}(1+z)^{6\alpha}}, \quad (2)$$

$$c_s^2 = -(2\alpha - 1)w_k, \quad (3)$$

where  $\alpha = n/(2n - 1)$  and  $k_0$  is a constant ( $-\infty < k_0 < +\infty$ , but because of the exponent 2, the case  $k_0 \geq 0$  and the case  $k_0 \leq 0$  are equivalent). Obviously, the EoS parameter is negative and not less than  $-1$ , meaning that the GTF does not violate the weak energy condition. For  $k_0 = 0$ , the EoS reduces to  $-1$ ; that is to say, the  $\Lambda$ CDM model is contained in the GTF dark energy scenario as one special case. As Eq. (3) shows,  $\alpha < 1/2$  will lead to imaginary sound speed and thus instabilities [21], so we will only concentrate on the case of  $\alpha > 1/2$  in the following. In this case, the behavior of the EoS (2), being  $\simeq -0$  in the early Universe, runs closely to  $-1$  in the future for  $k_0 \neq 0$ . Such behavior can, to a certain degree, solve the fine-tuning problem [22, 23].

There have been a number of papers considering observational constraints on GCG model, such as Refs. [24, 25, 26, 27, 28, 29, 30, 31, 32, 33, 34, 35, 36, 37, 38, 39, 40, 41, 42, 43, 44, 45, 46, 47, 48, 49, 50, 51, 52]. As the scalar field realization of GCG, GTF with Lagrangian (1) yet has not been fully analyzed with observational data currently available. This is necessary if such exotic types of matter are to be considered as serious alternatives to the  $\Lambda$ CDM scenario. Cosmological models that include (generalized) Chaplygin gas component can be divided into two classes: models with and without a significant CDM component.

It now appears increasingly likely from both theoretical stability issues and observational constraints (e.g. [24, 50, 51, 52]) from matter clustering properties (dark matter is very clumpy while dark energy is quite smooth out to the Hubble scale) that dark matter and dark energy are not the same substance. Also it appears rather difficult to unify dark matter and dark energy into a single scalar field in the context of the string landscape [53].

Nevertheless, in this paper we will consider these two cases: GTF as dark energy only and as unification of dark matter and dark energy, without loss of generality. The data sets used here include the recently released 182 gold supernova (SNIa) data [54], the shift parameter  $R$  and the acoustic scale  $l_a$  from observations of CMB [55]. Our results show that GTF dark energy scenario is favored over the  $\Lambda$ CDM model, and the  $\Lambda$ CDM model is favored over GTF as unification of dark matter and dark energy by the combined data.

## II. THE LUMINOSITY DISTANCE OF THE GTF MODEL

For a flat and homogeneous Friedmann-Robertson-Walker (FRW) space, the Einstein's field equations take the forms:

$$H^2 := \left(\frac{\dot{a}}{a}\right)^2 = H_0^2 E^2. \quad (4)$$

For GTF as dark energy component only

$$E(\Omega_m, k_0, \alpha) = [\Omega_m(1+z)^3 + \Omega_r(1+z)^4 + (1 - \Omega_m - \Omega_r)f(z)]^{1/2}, \quad (5)$$

where  $\Omega_m$  and  $\Omega_r$  are the present dimensionless density parameters of matter (including both the dark and baryonic matter) and radiation respectively;  $f(z)$  is the ratio of the energy density of GTF with respect to its present value  $f(z) \equiv \rho_k(z)/\rho_k(0) = \exp[3 \int_a^1 \frac{da'}{a'} (1 + w_k(a'))]$ . For GTF as unification of dark matter and dark energy

$$E(k_0, \alpha) = [\Omega_b(1+z)^3 + \Omega_r(1+z)^4 + (1 - \Omega_b - \Omega_r)f(z)]^{1/2}, \quad (6)$$

where  $\Omega_b$  is the present dimensionless density parameter of baryonic matter. The Hubble-parameter free luminosity distance is expressed as

$$D_L(z) = H_0(1+z) \int_0^{z'} \frac{dz'}{H}. \quad (7)$$

### III. OBSERVATIONAL CONSTRAINTS AND THE EVOLUTION OF THE GTF

To consider the best fit values of the parameters, we study observational bounds on the GTF models for a flat universe. Our constraints come from combinations of 182 gold supernova data [54] and the CMB observation [55].

The SNIa data which provide the main evidence for the existence of dark energy in the framework of standard cosmology [56]. Here we use a recently published dataset consisting of 182 SNIa with 23 SNIa at  $z \gtrsim 1$  obtained by imposing constraints  $A_v < 0.5$  (excluding high extinction) [54]. Each data point at redshift  $z_i$  includes the Hubble-parameter free distance modulus  $\mu_{\text{obs}}(z_i)$  ( $\equiv m_{\text{obs}} - M$ , where  $M$  is the absolute magnitude) and the corresponding error  $\sigma^2(z_i)$ . The resulting theoretical distance modulus  $\mu_{\text{th}}(z)$  is defined as

$$\mu_{\text{th}}(z) \equiv 5 \log_{10} D_L(z) + \mu_0, \quad (8)$$

where  $\mu_0 \equiv 5 \log_{10} h - 42.38$  is the nuisance parameter which can be marginalized over [57]. Fitting  $\Lambda$ CDM model with these 182 SNIa data, the best-fit value of parameter is  $\Omega_m = 0.34$ ; fitting GCG as dark energy component, it is  $\Omega_m = 0.39$  [27].

In order to break the degeneracies among the parameters, we consider the shift parameter  $R$  and the acoustic scale  $l_a$  [58] which are nearly uncorrelated with each other and defined as

$$R \equiv \Omega_m^{1/2} \int_0^{z_{\text{CMB}}} \frac{dz}{E(z)}, \quad (9)$$

$$l_a \equiv \frac{\pi \int_0^{z_{\text{CMB}}} dz/E(z)}{\int_0^{a_{\text{CMB}}} c_s da / (a\dot{a})}. \quad (10)$$

For the case of GTF as dark energy only,  $\Omega_r/\Omega_m = 1/(1 + z_{\text{eq}})(z_{\text{eq}} = 2.5 \times 10^4 \Omega_m h^2 (T_{\text{CMB}}/2.7\text{K})^{-4})$  with the redshift of recombination  $z_{\text{CMB}} = 1089$  ( $a_{\text{CMB}} = 1/[1 + z_{\text{CMB}}]$ ). The sound speed is  $c_s = 1/\sqrt{3(1 + R_b a)}$  with  $R_b a = 31500 \Omega_b h^2 (T_{\text{CMB}}/2.7\text{K})^{-4} a$ . COBE four year data give  $T_{\text{CMB}} = 2.728 \text{ K}$  [59]. For the case of GTF as unification of dark matter and dark energy,  $\Omega_m = \Omega_b + (1 - \Omega_b - \Omega_r)(1 + w_{k0})^{1/2\alpha}$  with  $w_{k0} = -1/(1 + 2k_0^{2\alpha})$  is the effective matter density parameter [42, 52], and  $\Omega_r = 10^{-5}$  is assumed. The three-year WMAP data give  $\Omega_b h^2 = 0.022 \pm 0.00082$ ,  $R = 1.70 \pm 0.03$  and  $l_a = 302.2 \pm 1.2$  [55]. Here we use the acoustic scale  $l_a$  with a prior of  $H_0 = 62.3 \pm 1.3$  (random)  $\pm 5.0$  (systematic) (km/s)  $\text{Mpc}^{-1}$  from HST Cepheid-calibrated luminosity of Type Ia SNIa observations recently [60].

The shift parameter  $R$  is a geometrical measure as it measures the size of apparent sound horizon at the epoch of recombination. Keeping the sound horizon size fixed, different cosmological models lead to different background expansion and hence the shift parameter can be used to compare and constrain different models. However, the sound horizon size also changes when varying cosmological parameters, most notably changing the matter density  $\Omega_m$ . Hence in general the shift parameter will not be an accurate substitute for CMB data, but the combination of the shift parameter  $R$  and the acoustic scale  $l_a$  has been proved to be a good and efficient approximation to the full CMB data to probe cosmological models [55, 61, 62].

Since the SNIa, the shift parameter  $R$ , and the acoustic scale  $l_a$  are effectively independent measurements, we can simply minimize their total  $\chi^2$  value given by [63, 64, 65]

$$\chi^2(\Omega_m, k_0, \alpha) = \chi_{\text{SNIa}}^2 + \chi_R^2 + \chi_{l_a}^2, \quad (11)$$

where

$$\chi_{\text{SNIa}}^2 = \sum_{i=1}^N \frac{(\mu_L^{\text{obs}}(z_i) - \mu_L^{\text{th}}(z_i))^2}{\sigma_i^2}, \quad (12)$$

$$\chi_R^2 = \left( \frac{R - 1.70}{0.03} \right)^2, \quad (13)$$

and

$$\chi_{l_a}^2 = \left( \frac{l_a - 302.2}{1.2} \right)^2, \quad (14)$$

in order to find the best fit values of the parameters of the GTF models.

### A. The case of GTF as dark energy only

For the case of GTF as dark energy component only, we obtain the best fit values of the parameters at 68% confidence level:  $\Omega_m = 0.37 \pm 0.01$ ,  $k_0 = 0.09_{-0.03}^{+0.04}$  and  $\alpha = 1.8_{-0.7}^{+7.4}$  with  $\chi_{k,\text{min}}^2 = 159.30$  ( $p(\chi^2 > \chi_{k,\text{min}}^2) = 0.88$ ), comparing with  $\Omega_m = 0.39 \pm 0.009$  and  $\chi_{\Lambda,\text{min}}^2 = 168.59$  ( $p(\chi^2 > \chi_{\Lambda,\text{min}}^2) = 0.77$ ) in the  $\Lambda$ CDM case. The probability of the improvement in the  $\chi_{\text{min}}^2$  by chance is 0.59% with F-statistic value of 5.28 resulted from F-test.

Now we apply information criteria to assess the strength of models. These statistics favor models that give a good fit with data. In this paper we use the Akaike Information Criterion

(AIC) [66] and the Bayesian Information Criterion (BIC) [67] (see also [68] and reference therein) to select the best-fit models. Comparing with the  $\Lambda$ CDM case, the difference of the Akaike Information Criterion (AIC) is  $\Delta\text{AIC} = -5.29$ , supporting GTF dark energy scenario; the Bayesian Information Criterion (BIC) is  $\Delta\text{BIC} = 1.14$ , less supporting GTF dark energy scenario.

Because model-comparison statistics can not discriminate between GTF dark energy scenario and the  $\Lambda$ CDM model. We carry out another independent observational test with 9  $H(z)$  data points [69, 70] in the range  $0 \lesssim z \lesssim 1.8$  obtained by using the differential ages of passively evolving galaxies determined from the Gemini Deep Deep Survey (GDDS) [71] and archival data [72, 73]. We compare these observational  $H(z)$  data with the predicted values of the Hubble parameter  $H$  of the GTF dark energy scenario for the case of ( $\Omega_m = 0.37$ ,  $k_0 = 0.09$ ,  $\alpha = 1.8$ ) and the case of ( $\Omega_m = 0.39$ ,  $k_0 = 0$ ) respectively. We find  $\chi^2 = 11.87$  ( $p(\chi^2 > 11.86) = 0.22$ ) for the former case and  $\chi^2 = 12.66$  ( $p(\chi^2 > 12.66) = 0.18$ ) for the latter case, both with 9 degrees of freedom because no fitting is done with the  $H(z)$  data. This serves as an independent evidence that the GTF dark energy scenario is favored over the  $\Lambda$ CDM model by these  $H(z)$  data. The predicted values of the Hubble parameter  $H$  of the GTF dark energy scenario in 68.3% confidence level limits compared with the observational  $H(z)$  data is shown in figure 1; the  $\Lambda$ CDM case is also presented for comparison.

Figures 2, 3, 4 show the 68.3%, 95.4% and 99.7% joint confidence contours in the  $\Omega_m$ - $k_0$  plane with  $\alpha$  at its best fit value of 1.8, the  $\Omega_m$ - $\alpha$  plane with  $k_0$  at its best fit value of 0.09, and the  $\alpha$ - $k_0$  plane with  $\Omega_m$  at its best fit value of 0.37 respectively. The dot-dashed lines, dotted lines, dashed lines represent the results from the 182 gold SNIa sample, the acoustic scale  $l_a$  and the shift parameter  $R$  respectively. The colored areas show the results from the combination of these three data sets. Obviously the current observational bounds on the index  $\alpha$  are considerably weak.

## B. The case of GTF as unification of dark matter and dark energy

For the case of GTF as unification of dark matter and dark energy, we find the best fit values of the parameters at 68% confidence level:  $k_0 = 0.21^{+0.2}_{-0.18}$  and  $\alpha = 0.57 \pm 0.01$  with  $\chi^2_{\text{k,min}} = 167.27$  ( $p(\chi^2 > \chi^2_{\text{k,min}}) = 0.78$ ).

For GTF as unification of dark matter and dark energy,  $k_0 = 0$  dose not correspond to

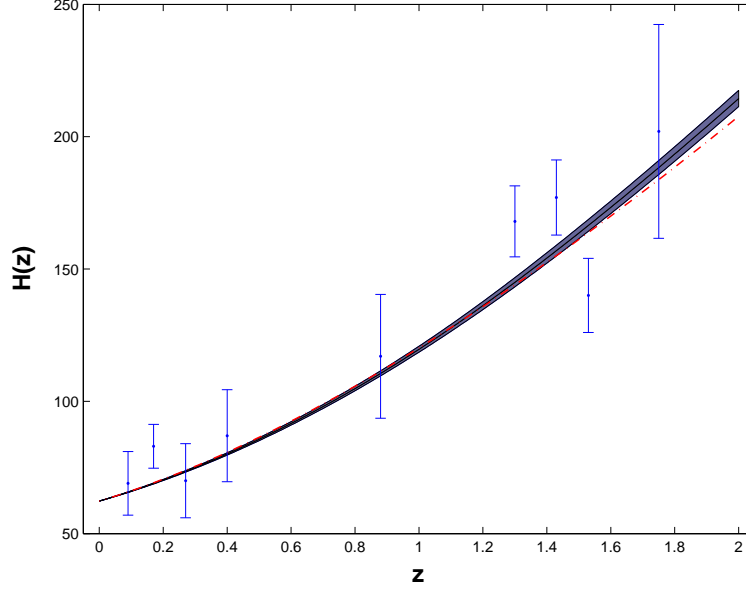


FIG. 1: The predicted values of the Hubble parameter  $H$  of the GTF as dark energy only in 68.3% confidence level limits from fitting the combined data, compared with the observational  $H(z)$  data with error bars and the  $\Lambda$ CDM case (the dash-dot line).

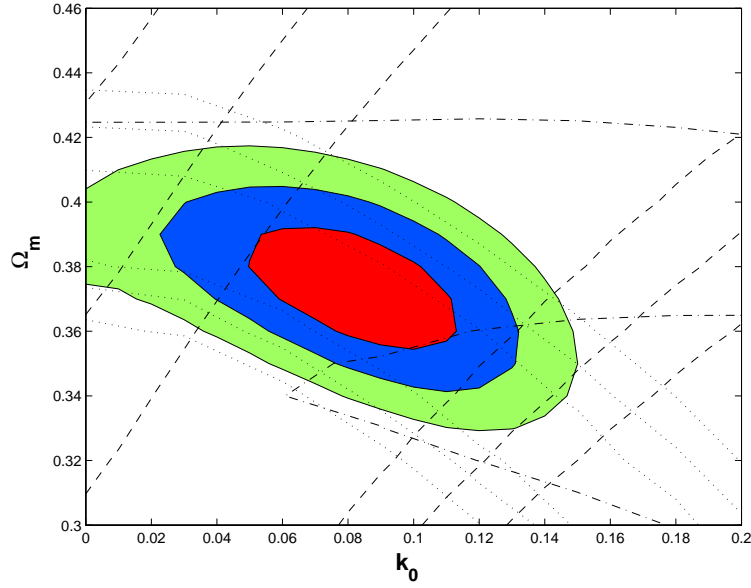


FIG. 2: The 68.3%, 95.4% and 99.7% confidence regions in the  $k_0$ - $\Omega_m$  plane with  $\alpha$  at its best-fit value of 1.8, for the case of GTF as dark energy only. The dot-dashed lines, dotted lines, dashed lines represent the results from the 182 gold SNIa sample, the acoustic scale and the shift parameter respectively. The colored areas show the results from the combination of these three data sets.

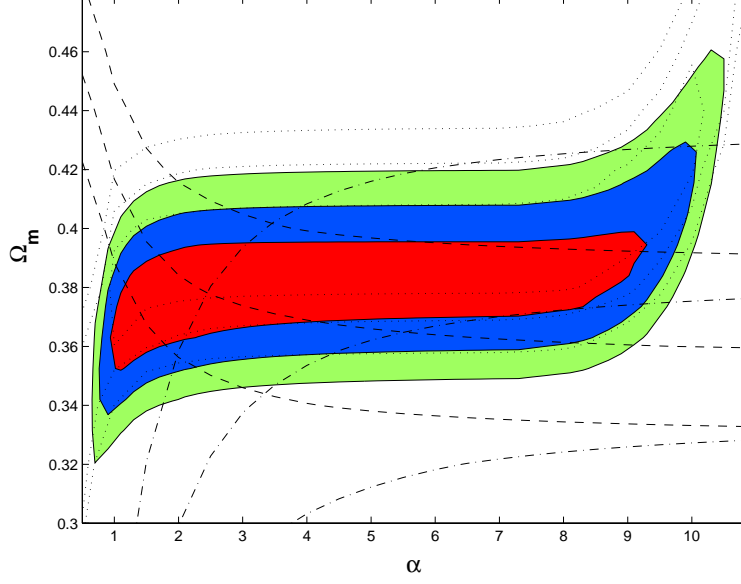


FIG. 3: The same confidence regions as in Fig 2 in the  $\alpha$ - $\Omega_m$  plane with  $k_0$  at its best-fit value of 0.09, for the case of GTF as dark energy only.

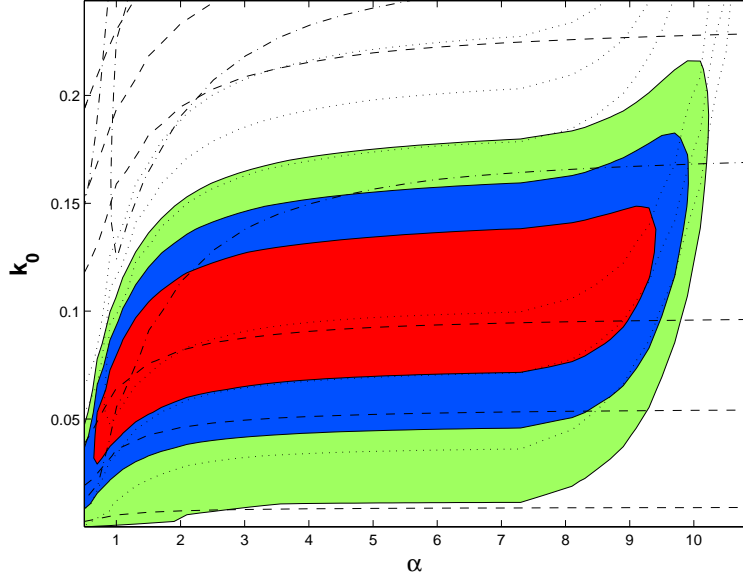


FIG. 4: The same confidence regions as in Fig 2 in the  $\alpha$ - $k_0$  plane with  $\Omega_m$  at its best-fit value of 0.37, for the case of GTF as dark energy only.

the  $\Lambda$ CDM case, so we can not apply F-test [74] for model selection, but we can still apply AIC and BIC. Comparing with the  $\Lambda$ CDM case, we find  $\Delta\text{AIC}=0.68$  and  $\Delta\text{BIC}=3.89$ . Comparing with the case of GTF as dark energy, we find  $\Delta\text{AIC}=5.97$  and  $\Delta\text{BIC}=2.8$ . These results of model-comparison statistics indicate that the case of GTF as unification of



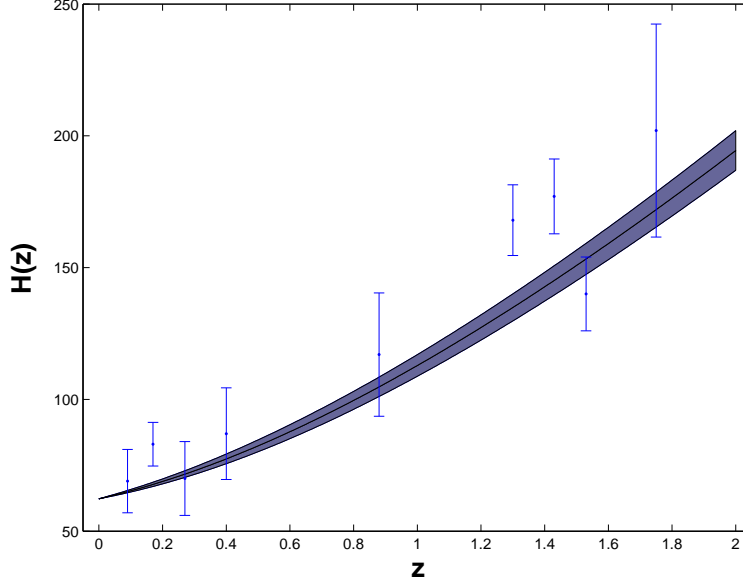


FIG. 5: The predicted values of the Hubble parameter  $H$  of GTF unification of dark matter and dark energy in 68.3% confidence level limits from fitting the combined data, compared with the observational  $H(z)$  data with error bars.

dark matter and dark energy is not favored by the combined data.

To confirm this result, we also carry out the independent 9  $H(z)$  data points [69, 70] test. We find  $\chi^2 = 16.60$  ( $p(\chi^2 > 11.86) = 0.06$ ), meaning that GTF as unification of dark matter and dark energy is also not favored by these  $H(z)$  data as shown in figure 5.

Figure 6 shows the 68.3%, 95.4% and 99.7% joint confidence contours in the  $\alpha$ - $k_0$  plane. The dot-dashed lines, dotted lines, dashed lines represent the results from the 182 gold SNIa sample, the shift parameter  $R$  and the acoustic scale  $l_a$  respectively. The colored areas show the results from the combination of these three data sets. Obviously the current observational bounds on the index  $k_0$  are considerably weak.

### C. The evolution of the GTF

To study the evolution of the GTF, we investigate the deceleration parameter  $q(z)$ , the EoS parameter  $w_k(z)$ , and the energy density  $\rho_k(z)$ . For GTF as dark energy component alone, the deceleration parameter  $q(z)$  is defined as

$$q(z) = -a\ddot{a}/\dot{a}^2 = \frac{1}{2}\Omega_m(z) + \frac{1 + 3w_k(z)}{2}\Omega_k(z), \quad (15)$$

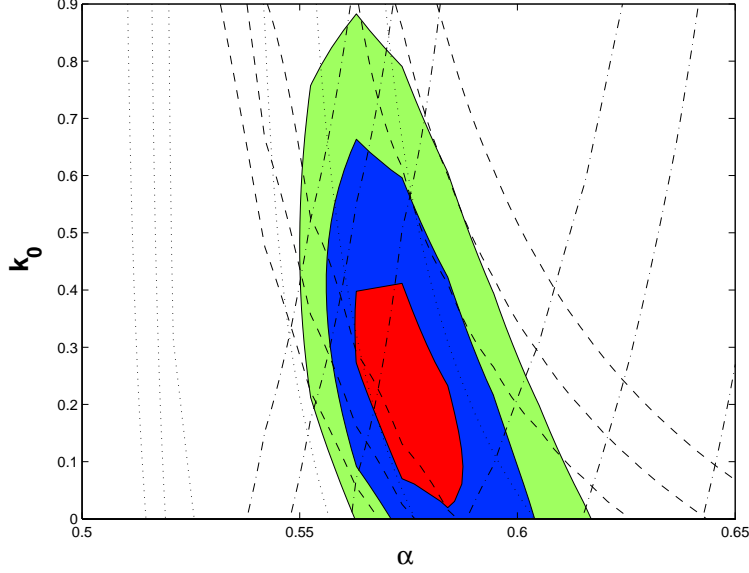


FIG. 6: The 68.3%, 95.4% and 99.7% confidence regions in the  $\alpha$ - $k_0$  plane, for the case of GTF as unification of dark matter and dark energy. The dot-dashed lines, dotted lines, dashed lines represent the results from the 182 gold SNIa sample, the shift parameter, and the acoustic scale respectively. The colored areas show the results from the combination of these three data sets.

where  $\Omega_k$  is energy density parameter of GTF. For GTF as unification of dark matter and dark energy, the deceleration parameter  $q(z)$  is given by

$$q(z) = \frac{1}{2}\Omega_b(z) + \frac{1 + 3w_k(z)}{2}\Omega_k(z), \quad (16)$$

Because we only consider the evolution of the deceleration parameter at low redshift, the radiation is ignored here.

For the case of GTF as dark energy component only, the present value of the deceleration parameter  $q(z)$  is found to be  $-q_{z=0} \sim 0.44 - 0.48$ . The phase transition from deceleration to acceleration of the Universe occurs at the redshift  $z_{q=0} \sim 0.47 - 0.51$  in 68.3% confidence level limits, as shown in figure 7. For GTF as unification of dark matter and dark energy,  $-q_{z=0} \sim 0.50 - 0.61$  and  $z_{q=0} \sim 0.49 - 0.68$  in 68.3% confidence level limits as shown in figure 8. All these results are comparable with that estimated from 157 gold data ( $z_t \simeq 0.46 \pm 0.13$ ) [75], but less than that obtained from gold+SNLS SNIa data for DGP brane ( $z_{q=0} \sim 0.8 - 0.93$ ) [76].

For the case of GTF as dark energy component only, figure 9 and 10 show the evolution of the EoS parameter and the energy density ratio of GTF dark energy at low or high

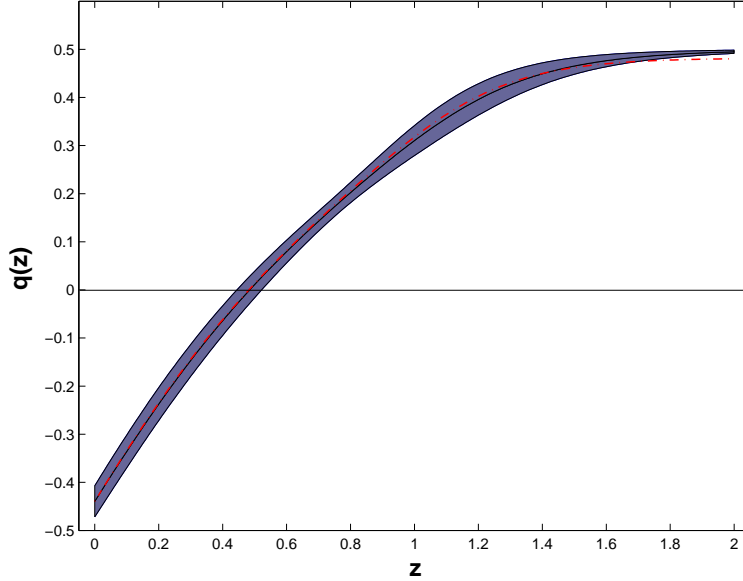


FIG. 7: The deceleration parameter as a function of redshift in 68.3% confidence level limits from fitting the combined data, compared with the  $\Lambda$ CDM case (the dash-dot line), for GTF as dark energy component only.

redshift, compared with the vacuum energy in both cases. For  $z \gtrsim 2$ , the EoS parameter runs closely to  $-0$ , meaning the negative pressure of the GTF dark energy approaches to zero rapidly, compared with the cases of the radiation and the dark matter. Such behavior can, to a certain degree, solve the fine-tuning problem [22, 23]. For GTF as unification of dark matter and dark energy, figure 11 and 12 show the evolution of the EoS parameter and the energy density ratio at low or high redshift, compared with the cases of the radiation and the vacuum energy. All these results at low redshift are consistent with that obtained in Ref. [55] by model-independent methods in 68.3% confidence level limits.

#### IV. GROWTH OF LINEAR DENSITY PERTURBATIONS

Stability properties of some perfect fluid cosmological models are studied extensively [77], such as Refs. [16, 50, 51, 52, 78, 79] concentrated on the stability of GCG as unification of dark matter and dark energy, Refs. [24, 27, 80] on the stability of GCG as dark energy component only, and Refs. [17, 81, 82] on the stability of tachyon field dark energy.

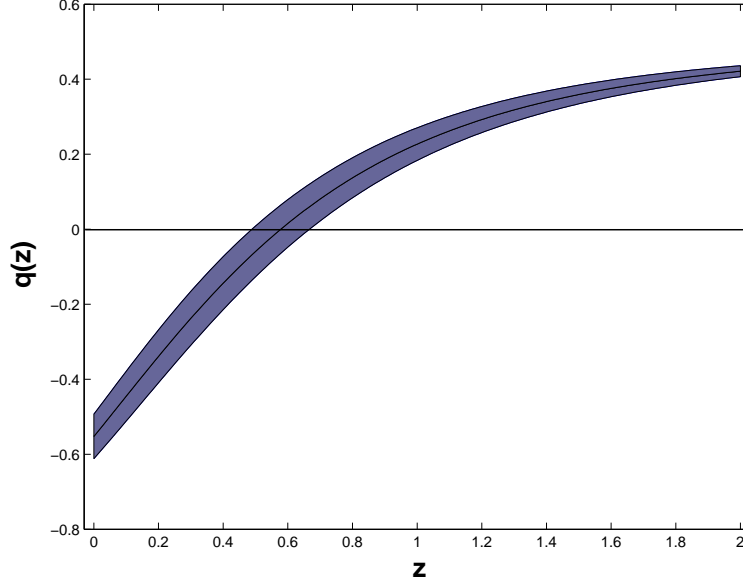


FIG. 8: The deceleration parameter as a function of redshift in 68.3% confidence level limits from fitting the combined data, for GTF as unification of dark matter and dark energy.

#### A. The case of GTF as dark energy only

In this subsection, we study the growth of density perturbations for the mixture of a matter fluid and a GTF dark energy fluid in the linear regime on subhorizon scales. Assuming the GTF dark energy to be a smooth, unclustered component (the only effect of the GTF evolution is to alter the growth of matter perturbations through the effect of the GTF energy density on the expansion of the universe), the growth equation for the linear matter density perturbation,  $\delta \equiv \delta\rho_m/\rho_m$ , is given by [27, 80]

$$\delta'' + \left(2 + \frac{\dot{H}}{H^2}\right) \delta' + 3c_1\delta = 0, \quad (17)$$

where “prime” denotes the derivative with respect to  $\ln a$ , “dot” denotes the derivative with respect to  $t$ ,  $H$  is the Hubble parameter for the background expansion gives in Eq. (4), and  $c_1$  is given by

$$c_1 = -\frac{1}{2} \frac{\Omega_m}{\Omega_m + \Omega_k[1 + w_{k0}(a^{6\alpha} - 1)]^{1/2\alpha}}, \quad (18)$$

with  $w_{k0} = 1/(1 + 2k_0^{2\alpha})$ . For  $k_0 = 0$ , the equation reduces to that for the  $\Lambda$ CDM model. The initial conditions are chosen such that at  $a = 10^{-3}$ , the standard solution  $\delta \sim a$  for Einstein-deSitter universe is reached. We have integrated Eq. (17) numerically from  $a = 10^{-3}$  to

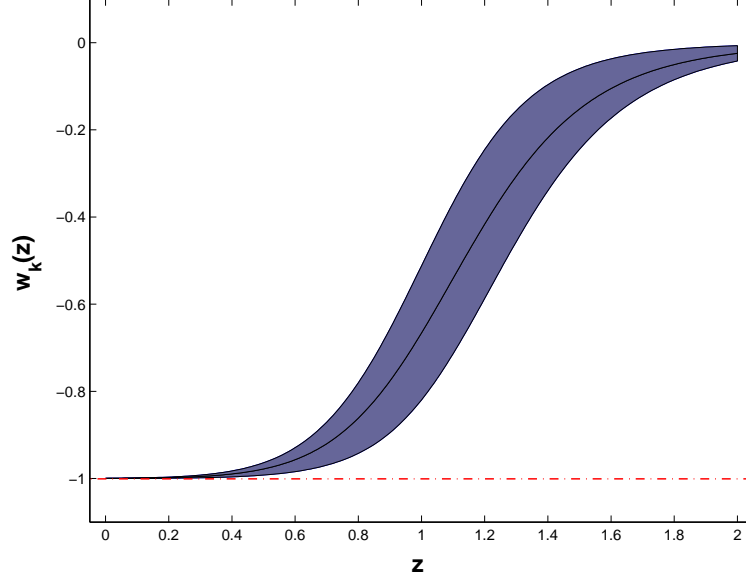


FIG. 9: The evolution of the equation of state parameter of GTF as dark energy component only in 68.3% confidence level limits from fitting the combined data, compared with the  $\Lambda$ CDM case (the dash-dot line).

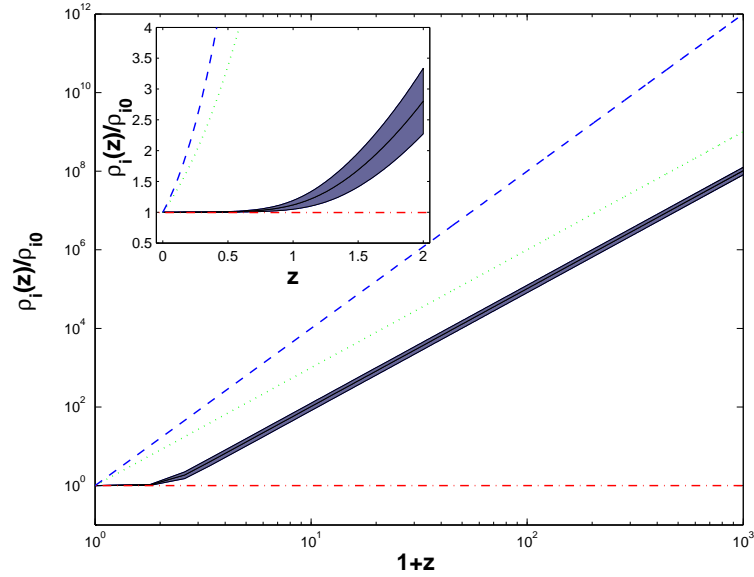


FIG. 10: The evolution of the energy density ratio of the GTF as dark energy component only in 68.3% confidence level limits from fitting the combined data, compared with the cases of the radiation (the dash line), the dark matter (the dot line), and the vacuum energy (the dash-dot line).

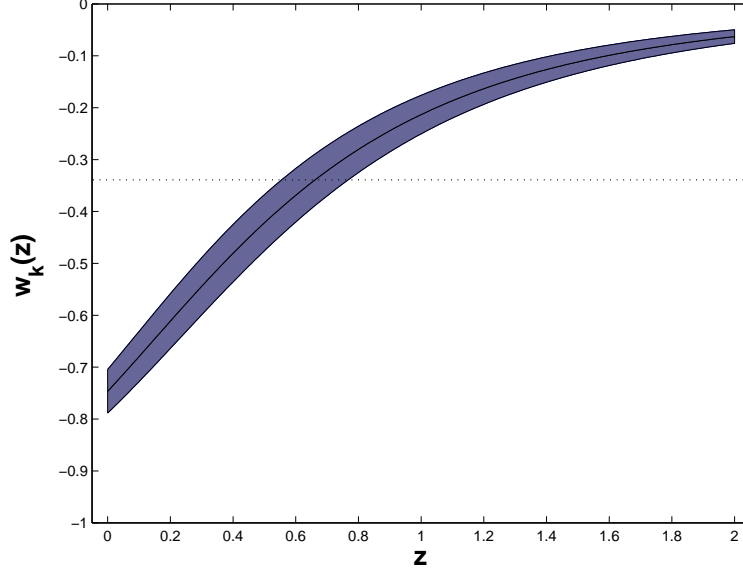


FIG. 11: The evolution of the equation of state parameter of GTF as unification of dark matter and dark energy in 68.3% confidence level limits from fitting the combined data.

$a = 1$  for some selected values of the parameters ( $k_0$  and  $\alpha$ ) in 68% confidence level. Figure 13 shows the behavior of  $\delta$  as a function of the scale factor. Compared to the  $\Lambda$ CDM universe, fluctuations grow more slowly in a universe where GTF dark energy plays a role. For parameters ( $k_0$  and  $\alpha$ ) changing in 68% confidence level,  $\delta$  deviates slightly, consistent with the growth of linear density perturbations. The behavior of  $\delta$  in Fig. 13 agrees with the result obtained in Ref. [27] in the framework of GCG dark energy.

### B. The case of GTF as unification of dark matter and dark energy

Because baryons play a crucial role in the context of unified dark matter/dark energy models [83, 84], here we study the growth of density perturbations for the mixture of a baryonic fluid and a GTF fluid unifying dark matter and dark energy. In the comoving synchronous gauge the relativistic equations governing the evolution of perturbations in a two fluid (baryon and GTF) system are [83, 85]

$$\delta_b'' + \left(2 + \frac{\dot{H}}{H^2}\right) \delta_b' + \frac{3}{2} [\Omega_b \delta_b + (1 - 3(2\alpha - 1)w_k)\Omega_k \delta_k] = 0, \quad (19)$$

$$\delta_k' + (1 + w_k)[\theta_k/aH - \delta_b'] - 6\alpha w_k \delta_k = 0, \quad (20)$$

$$\theta_k' + [1 + 3(2\alpha - 1)w_k]\theta_k + \frac{(2\alpha - 1)w_k k^2}{aH(1 + w_k)} \delta_k = 0, \quad (21)$$

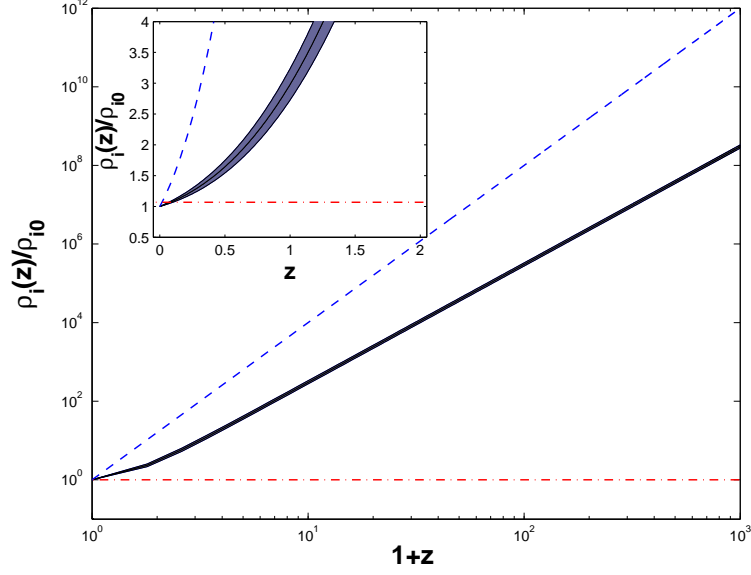


FIG. 12: The evolution of the energy density ratio of the GTF as unification of dark matter and dark energy in 68.3% confidence level limits from fitting the combined data, compared with the cases of the radiation (the dash line) and the vacuum energy (the dash-dot line).

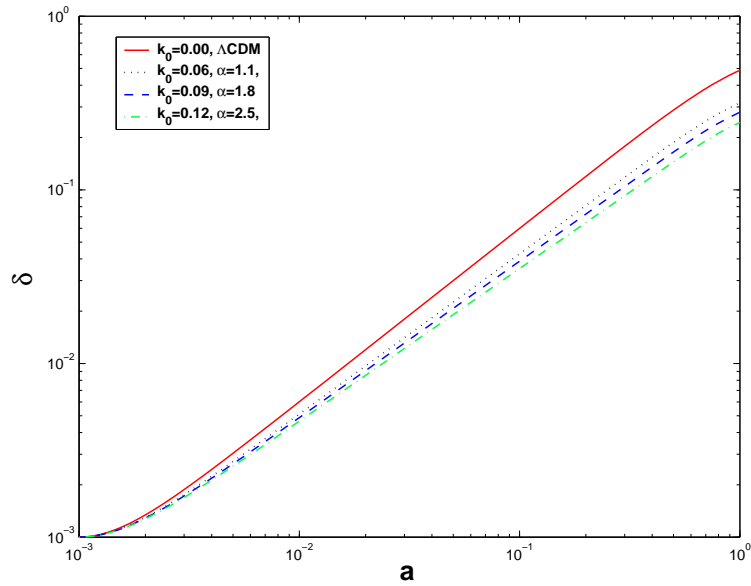


FIG. 13: The evolution of the matter density perturbation  $\delta$  as a function of the scale factor  $a$  (normalized to  $a = 1$  at the present) for some selected values of the parameters ( $k_0$  and  $\alpha$ ) of the GTF as dark energy in 68% confidence level with  $\Omega_m = 0.37$ .

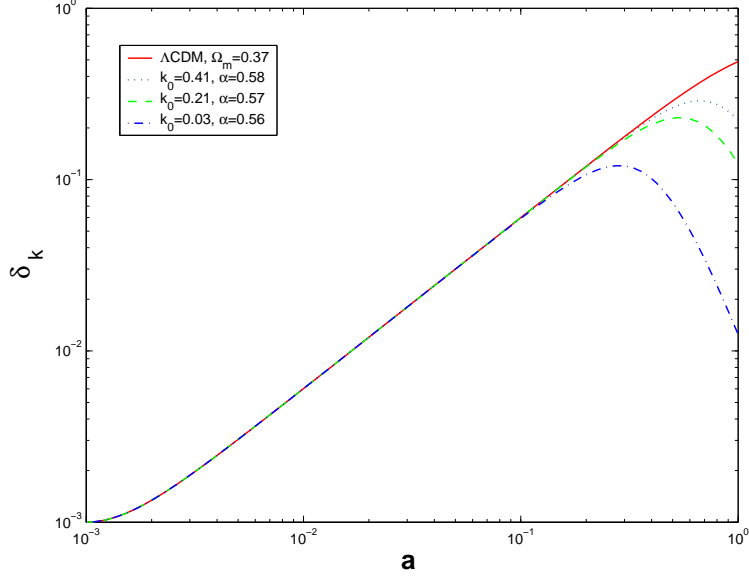


FIG. 14: The evolution of the GTF (unified dark matter) density perturbation  $\delta_k$  as a function of the scale factor  $a$  (normalized to  $a = 1$  at the present) for some selected values of the parameters ( $k_0$  and  $\alpha$ ) in 68% confidence level, compared with the evolution of the matter density perturbation  $\delta$  in the case of  $\Lambda$ CDM.

where  $\delta_i''$  is the density contrast of the  $i$ th fluid obeying  $p_i = w_i \rho_i$ ,  $\theta_k$  is element velocity divergence. Given  $w_k$  and  $H$  as functions of  $a$  we can easily transform this set of equations into four first order differential equations and integrate them using numerical method. Since in the linear regime and deep into the matter era  $\delta_i \propto a$  implying  $\delta_i' \propto a$  with normalized initial conditions  $[\delta_b, \delta_b', \delta_k, \theta] = [0.001, 0.001, 0.001, 0]$  for  $a = 0.001$  and a prior  $k = 100h$   $\text{Mpc}^{-1}$  which corresponds to a scale of order  $50h^{-1}\text{kpc}$ . Figure 14 shows the behavior of  $\delta_k$  as a function of the scale factor. The fluctuations of GTF density grow more slowly for  $a \rightarrow 1$ , meaning GTF does not behave as classical  $\Lambda$ CDM scenarios. The reason is that baryons can carry over gravitational clustering when the GTF fluid starts behaving differently from CDM [83].

## V. CONCLUSIONS AND DISCUSSIONS

Assuming that the Universe is spatially flat, we place observational constraints on GTF scenario with 182 gold SNIa data and two cosmic microwave background parameters (the shift parameter and the acoustic scale). For GTF as dark energy component only, the best-fit



values of the parameters at 68.3% confidence level are:  $\Omega_m = 0.37 \pm 0.01$ ,  $k_0 = 0.09^{+0.04}_{-0.03}$  and  $\alpha = 1.8^{+7.4}_{-0.7}$  with  $\chi^2_{k,\min} = 159.30$  ( $p(\chi^2 > \chi^2_{k,\min}) = 0.88$ ), comparing with  $\chi^2_{\Lambda,\min} = 168.59$  ( $p(\chi^2 > \chi^2_{\Lambda,\min}) = 0.77$ ) in the  $\Lambda$ CDM case. For GTF as unification of dark matter and dark energy, the best fit values of the parameters at 68% confidence level are:  $k_0 = 0.21^{+0.2}_{-0.18}$  and  $\alpha = 0.57 \pm 0.01$ , with  $\chi^2_{k,\min} = 167.27$  ( $p(\chi^2 > \chi^2_{k,\min}) = 0.78$ ). In both cases, GTF evolves like dark matter in the early universe.

To consider the best-fit models, we apply model-comparison statistics. Comparing with GTF dark energy scenario, the combined data do not support the  $\Lambda$ CDM case according to F-test and AIC, but possibly support the  $\Lambda$ CDM case according to BIC. Similarly the case of GTF as unification of dark matter and dark energy is not supported according to F-test, AIC and BIC. Tested with independent 9  $H(z)$  data points, GTF dark energy scenario is favored over the  $\Lambda$ CDM model, and the  $\Lambda$ CDM model is favored over GTF as unification of dark matter and dark energy. This supports theoretical arguments against unifying dark matter and dark energy into one scalar field. Of course, new and better data are still needed to further discriminate between these models.

By investigating the deceleration parameter, we find that the present value of the deceleration parameter  $q(z)$  is  $-q_{z=0} \sim 0.44 - 0.48$ , the phase transition from deceleration to acceleration of the Universe occurs at the redshift  $z_{q=0} \sim 0.47 - 0.51$  in 68.3% confidence level limits for GTF as dark energy component only; and  $-q_{z=0} \sim 0.50 - 0.61$  and  $z_{q=0} \sim 0.49 - 0.68$  in 68.3% confidence level limits for GTF as unification of dark matter and dark energy. These results can be tested with future cosmological observations. If assumed to be a smooth component, GTF as dark energy component is consistent with the growth of linear density perturbations. If GTF unifies dark matter and dark energy, because baryons can carry over gravitational clustering when the GTF fluid starts behaving differently from CDM, the growth of GTF density fluctuations grow more slowly for  $a \rightarrow 1$ , meaning GTF do not behave as classical  $\Lambda$ CDM scenarios.

## Acknowledgments

We thank Yun Wang, Zu-Hui Fan, Hao Wei, Pu-Xun Wu, Yan Wu, Wei-Ke Xiao, Jian-Feng Zhou, Zhi-Xing Ling, and Bi-Zhu Jiang for discussions. The anonymous referee is thanked for his/her patience in reviewing this manuscript several times, as well as providing

insightful and constructive criticisms and suggestions, which allowed us to improve the manuscript significantly. This study is supported in part by the Ministry of Education of China, Directional Research Project of the Chinese Academy of Sciences under project No. KJCX2-YW-T03 and by the National Natural Science Foundation of China under project no. 10521001, 10733010 and 10725313.

---

- [1] Sen A 2002 Mod. Phys. Lett. A **17** 1797; 2005 Int. J. Mod. Phys. A **20** 5513
- [2] Padmanabhan T and Choudhury T R 2002 Phys. Rev. D **66**, 081301
- [3] Gorini V, Kamenshchik A, Moschella U and Pasquier V 2004 Phys. Rev. D **69**, 123512
- [4] Shao Y, Gui Y.-X. and Wang W 2007 MPLA **22** 1175
- [5] Choudhury D, Ghoshal D, Jatkar D P and Panda S 2002 Phys. Lett. B **544**, 231.
- [6] Hao J and Li X 2002 Phys. Rev. D **66**, 087301
- [7] Bagla J S, Jassal H K and Padmanabhan T 2003 Phys. Rev. D **67**, 063504
- [8] Calcagni G and Liddle A R 2006 Phys. Rev. D **74**, 043528
- [9] Garousi M R, Sami M and Tsujikawa S 2004 Phys. Rev. D **70**, 043536
- [10] Copeland E J, Garousi M R, Sami M and Tsujikawa S 2005 Phys. Rev. D **71**, 043003
- [11] Cardenas V H 2006 Phys. Rev. D **73**, 103512
- [12] Shiu G and Wasserman I 2002 Phys. Lett. B **541**, 6
- [13] Wang Y and Mukherjee P 2006 Astrophys. J. **650**, 1
- [14] Koshelev A S 2007 Journal of High Energy Physics, 04, 029
- [15] Chimento L P 2004 Phys. Rev. D **69** 123517
- [16] Gorini V, Kamenshchik A, Moschella U, Pasquier V and Starobinsky A 2005 Phys. Rev. D **72**, 103518
- [17] Frolov A, Kofman L and Starobinsky A 2002 Phys. Lett. B **545**, 8
- [18] Kamenshchik A, Moschella U and Pasquier V 2001 Phys. Lett. B **511**, 265
- [19] Scherrer R J 2004 Phys. Rev. Lett. **93** 011301
- [20] Yang R J and Zhang S N 2008 Chin. Phys. Lett. **25** 344
- [21] Garriga J and Mukhanov V F 1999 Phys. Lett. B **458** 219
- [22] Armendáriz-Picón C, Mukhanov V, and Steinhardt P J 2000 Phys. Rev. Lett. **85** 4438; 2001 Phys. Rev. D **63** 103510.

- [23] Chiba T, Okabe T, and Yamaguchi M 2000 Phys. Rev. D **62** 023511
- [24] Bean R and Doré O 2003 Phys. Rev. D **68** 023515.
- [25] Gorini V, Kamenshchik A and Moschella U 2003 Phys. Rev. D **67**, 063509  
Gorini V, Moschella U, Kamenshchik A and Pasquier V 2005 AIP Conf. Proc. **751** 108
- [26] Colistete R Jr, Fabris J C, Gonalves S V B and de Souza P E 2003 Int. J. Mod. Phys. D **13** 669
- [27] Sen A A and Scherrer R J 2005 Phys. Rev. D **72** 063511
- [28] Multamäki T, Manera M and Gaztanaga E 2004 Phys. Rev. D **69** 023004
- [29] Makler M, Oliveira S Q and Waga I 2003 Phys. Lett. B **555** 1
- [30] Silva P T and Bertolami O 2003 Astrophys. J. **599** 829
- [31] Cunha J V, Lima J A S and Alcaniz J S 2004 Phys. Rev. D **69** 083501
- [32] Bertolami O, Sen A A, Sen S and Silva P T 2004 Mon. Not. R. Astron. Soc. **353** 329
- [33] Zhu Z-H 2004 Astron. Astrophys. **423** 421
- [34] Zhang X, Wang F-Q and Zhang J-F 2006 J. Cosmol. Astropart. Phys. JCAP01(2006)003
- [35] Bouhmadi-Lopez M and Jimenez Madrid J A 2005 J. Cosmol. Astropart. Phys. JCAP05(2005)005
- [36] Gong Y-G 2005 J. Cosmol. Astropart. Phys. JCAP03(2005)007
- [37] Giannantonio T and Melchiorri A 2006 Class. Quantum Grav. **23** 4125
- [38] Biesiada M, Godlowski W and Szydlowski M 2005 Astrophys. J. **622** 28
- [39] Jimenez Madrid J 2006 Phys. Lett. B **634** 106
- [40] Ghosh S, Kulkarni S and Banerjee R 2007 Phys. Rev. D **75** 025008
- [41] Lobo F S N 2006 Phys. Rev. D **73** 064028
- [42] Wu P and Yu H 2007 J. Cosmol. Astropart. Phys. JCAP03(2007)015; 2007 Astrophys. J. **658**, 663
- [43] Bento M C, Bertolami O and Sen A A 2003 Phys. Rev. D **67**, 063003
- [44] Alcaniz J, Jain D and Dev A 2003 Phys. Rev. D **67** 043514
- [45] Bertolami O and Silva P T 2006 Mon. Not. R. Astron. Soc. **365** 1149
- [46] Dev A, Jain D and Alcaniz J S 2003 Phys. Rev. D **67** 023515
- [47] Chen D M 2003 Astrophys. J. **587** L55; 2003 Astron. Astrophys. 397 415
- [48] Bilic N, Tupper G B and Viollier R D 2002 Phys. Lett. B **535** 17
- [49] Alcaniz J S, Jain D and Dev A 2003 Phys. Rev. D **67** 043514

- [50] Sandvik H, Tegmark M, Zaldarriaga M and Waga I 2004 Phys. Rev. D **69** 123524
- [51] Perrotta F, Matarrese S and Torki M 2004 Phys. Rev. D **70** 121304
- [52] Amendola L, Waga I and Finelli F 2005 J. Cosmol. Astropart. Phys. JCAP11(2005)009
- [53] Liddle A R and Ureña-López L A 2006 Phys. Rev. Lett. **97** 161301
- [54] Riess A G *et al* 2007 Astrophys. J. **659** 98
- [55] Wang Y and Mukherjee P 2007 astro-ph/0703780v1  
Wang Y 2006 Astrophys. J. **650** 1
- [56] Riess A G *et al* 1998 Astron. J. **116** 1009  
Perlmutter S *et al* 1999 Astrophys. J. **517** 565
- [57] Perivolaropoulos L 2005 Phys. Rev. D **71** 06350  
Pietro E Di and Claeskens J F 2003 Mon. Not. Roy. Astron. Soc. **341** 1299  
Gao C J and 2004 Phys.Rev. D **70** 124019  
Yang R J and Jing J L 2004 Chin. Phys. **5** 13; 2004 Chin. Phys. Lett. **3** 21  
Wei H and Zhang S N 2007 Phys. Rev. D **75** 043009
- [58] Page L *et al* 2003 Astrophys. J. Suppl. **148** 233
- [59] Fixsen D J 1996 Astrophys. J. **473** 576
- [60] Sandage A *et al* 2006 Astrophys. J. **653**, 843
- [61] Elgarøy O and Multamäki T 2007 Astron. Astrophys. **471** 65
- [62] Wright E L 2007 Astrophys. J. **664** 633
- [63] Movahed M S and Rahvar S 2006 Phys. Rev. D **73** 083518  
Nesseris S and Perivolaropoulos L 2004 Phys. Rev. D **70** 043531
- [64] Wu P and Yu H 2007 Phys. Lett. B **644** 16
- [65] Wei H and Zhang S N 2007 Phys. Rev. D **76** 063003; 2007 Phys. Lett. B **644** 7; 2007 Phys. Lett. B **654** 139
- [66] Akaike H 1974 IEEE Transactions on Automatic Control **19** 716
- [67] Schwarz G 1978 The Annals of Statistics **6** 461
- [68] Liddle A R 2004 MNRAS **351** L49
- [69] Jimenez R, Verde L, Treu T and Stern D 2003 Astrophys. J. **593** 622
- [70] Simon J, Verde L and Jimenez R 2005 Phys. Rev. D **71** 123001
- [71] Abraham R G *et al* 2004 Astron J **127** 2455
- [72] Treu T, Stiavelli M, Casertano S, Moller P and Bertin G 1999 Mon. Not. Roy. Astron. Soc.

- 308** 1037
- Dunlop J, Peacock J, Spinrad H, Dey A, Jimenez R, Stern D and Windhorst R 1996 *Nature* **381** 581
- Spinrad H, Dey A, Stern D, Dunlop J, Peacock J, Jimenez R and Windhorst R 1997 *Astrophys J* **484** 581
- Nolan L A, Dunlop J S, Jimenez R and Heavens A F 2003 *Mon. Not. Roy. Astron. Soc.* **341** 464
- [73] Samushia L and Ratra B 2006 *Astrophys. J.* **650** L5
- [74] Protassov R and van Dyk D A 2002 *Astrophys. J.* **571** 545
- [75] Riess A G *et al* 2004 *Astrophys. J.* **607** 665
- [76] Guo Z-K, Zhu Z-H, Alcaniz J S, Zhang Y-Z 2006 *Astrophys. J.* **646** 1
- [77] Bruni M, Dunsby P K S and Ellis G F R 1992 *Astrophys. J.* **395** 34
- Ma C-P, Bertschinger E 1995 *Astrophys. J.* **455** 7
- Bardeen J M 1980 *Phys. Rev. D* **22** 1882
- Giovannini M 2005 *Class. Quantum Grav.* **22** 5243
- Perrotta F, Matarrese S, Pietroni M and Schimd C 2004 *Phys. Rev. D* **69** 084004
- Casadio R, Finelli F, Kamenshchik A, Luzzi M and Venturi G 2006 *J. Cosmol. Astropart. Phys.* JCAP04(2006)011
- [78] Zimdahl W and Fabris J C 2005 *Class. Quantum Grav.* **22** 4311
- [79] Avelino P P Beça L M G, de Carvalho J P M, Martins C J A P and Pinto P 2003 *Phys. Rev. D* **67** 023511
- [80] Multamäki M, Manera M and Gaztañaga E 2004 *Phys. Rev. D* **69** 023004
- [81] Jain R K, Chingangbam P and Sriramkumar L 2007 *J. Cosmol. Astropart. Phys.* JCAP10(2007)003
- [82] Raul Abramo L and Finelli F 2003 *Phys. Lett. B* **575** 165
- [83] Beça L M, Avelino P P, de Carvalho J P and Martins C J 2003 *Phys. Rev. D* **67** 101301
- [84] Gorini V, Kamenshchik A Y, Moschella U, Piattella O F and Starobinsky A A 2007 *astro-ph* arXiv:0711.4242
- [85] Veeraraghavan S and Stebbins A 1990 *Astrophys. J.* **365** 37